to its composition $C_{24}H_{23}N_2OPS_8Ru$, dissolves readily in organic solvents like dichloromethane, acetonitrile, and dimethylformamide, leading to stable solutions for hours at room temperature. The IR and Raman bands and their assignments are given in Table IV. All bands are in the expected region.

The diamagnetism of **1** is typical for an $\{RuNO\}^6$ system which gives rise to low-spin configurations. The positions of a broad band centered at 440 nm and another intense band at 350 nm in the electronic absorption spectrum (solid-state reflectance) are approximately similar to those observed in the case of *cis*-$[Ru(NH_3)_4(NO)Cl]Cl_2$.[16]

The mass spectrum of the compound shows typically the fragmentation pattern of NH_3, with ion peaks corresponding to mass numbers 15, 16, and 17 besides all those expected from two S_4^{2-} groups.

It would be interesting to study the relation between the number of active sites on RuS_2 surfaces with different dispersions, determined by "titration" with NO, and HDS activity. This would answer the question of whether the Ru atoms or the S_2^{2-} groups are the active sites for the HDS process. In the case of promoted-HDS catalysts, an IR investigation of NO adsorption showed that the amount of NO adsorbed on cobalt edge atoms ("Co-Mo-S" atoms) is directly related to the promotion of catalytic activity.[10] The model for the nitrosylated HDS catalyst, $[Co(MoS_4)(NO)_2]^-$, exhibits ν(NO) bands with practically the same frequencies as those of the nitrosylated catalyst at the Co centers (for $[(NO)Mo(NCS)_4]^{2-}$ as corresponding model for the Mo centers, see refs 10 and 17) itself.[10]

Note Added in Proof. More evidence for the high activity of RuS_2 catalysts has been obtained in the meantime (Vrinat, M.; Lacroix, M.; Breysse, M.; Mosoni, L.; Roubin, M. *Catal. Lett.* **1989**, *3*, 405. De los Reyes, J. A.; Göbölös, S.; Vrinat, M.; Breysse, M. *Catal. Lett.* **1990**, *5*, 17. Yuan, S.; Decamp, T.; Lacroix, M.; Mirodatos, C.; Breysse, M. Submitted for publication in *J. Catal.*).

Acknowledgment. We thank the German Academic Exchange Service for a fellowship (to M.I.K.). Financial assistance from the Westfälisch Lippische Universitätsgesellschaft and a gift of platinum metals from Degussa AG are gratefully acknowledged.

Supplementary Material Available: Crystal data (Table S1), bond lengths (Table S2), bond angles (Table S3), anisotropic thermal parameters (Table S4), and H atom coordinates with isotropic thermal parameters for **1** (Table S5) (7 pages); tables of calculated and observed structure factors (24 pages). Ordering information is given on any current masthead page.

(16) Pell, S.; Armor, J. N. *Inorg. Chem.* **1973**, *12*, 873.

(17) Müller, A. *Polyhedron* **1986**, *5*, 323.

Contribution from the Departamento de Química Inorgánica, Facultad de Ciencias, Universidad de Málaga, Apartado 59, 29071 Málaga, Spain, and Chemical Crystallography Laboratory, University of Oxford, 9 Parks Road, Oxford OX1 3PD, U.K.

Crystal Structures and Characterization of a New Manganese(III) Arsenate, $MnAsO_4 \cdot 1.2H_2O$, and Manganese(II) Pyroarsenate, $Mn_2As_2O_7$

Miguel A. G. Aranda,[1a] Sebastian Bruque,*[1a] and J. Paul Attfield[1b]

Received September 6, 1990

The synthesis and crystal structure of a new manganese(III) arsenate, $MnAsO_4 \cdot 1.2H_2O$, are reported. This compound crystallizes in a monoclinic space group, $C2/c$ (a = 7.030 (1) Å, b = 7.824 (1) Å, c = 7.469 (1) Å, β = 112.14 (1)°, Z = 4) and is isostructural with $MnPO_4 \cdot H_2O$. The structure has been refined from laboratory X-ray powder diffraction data by the Rietveld method (R_I = 3.3%, R_{WP} = 11.0%) and even the H position has been refined without constraints, showing that the water molecule is hydrogen-bonded to the arsenate groups. Whether the additional 0.2 water molecules are also present in the structure or in a second amorphous phase is unclear. A strong Jahn-Teller effect was found, in agreement with the diffuse-reflectance spectrum, and the TGA-DTA curves and the IR spectrum of the manganese(III) arsenate hydrate are discussed. The thermal decomposition product of $MnAsO_4 \cdot 1.2H_2O$, manganese(II) pyroarsenate, $Mn_2As_2O_7$, crystallizes with a thortveitite-type structure (a = 6.7493 (8) Å, b = 8.7589 (8) Å, c = 4.7991 (5) Å, β = 102.83 (1)°, Z = 2, space group $C2/m$) and has been refined (R_I = 2.9%, R_{WP} = 6.7%) with a split-site model to take account of the disorder of the bridging oxygen due to bending of the pyroarsenate groups.

Introduction

Phosphates and arsenates of the first-row transition metals adopt a wide variety of stoichiometries and structure types and have been studied for their properties and applications. For instance, they may be used as catalysts, nonlinear optical materials, ionic exchangers, ionic conductors, and host compounds for intercalation reactions.

No synthetic or structural works have been reported on any manganese(III) arsenates, but some studies on manganese(III) phosphates have been published. The structure of $MnPO_4 \cdot H_2O$ was determined from high-resolution synchrotron X-ray powder diffraction data,[2] and this compound has recently been studied by spectroscopic methods.[3] The crystal structures of the mixed-valence mineral bermanite, $Mn_3(PO_4)_2(OH)_2 \cdot 4H_2O$,[4] manganese(III) metaphosphate, $Mn(PO_3)_3$,[5] manganese(III) hydrogen pyrophosphate, $MnHP_2O_7$,[6] and two layered phosphates of manganese(III), $KMn_2O(PO_4)(HPO_4)$[7] and $NH_4Mn_2O(PO_4)(HPO_4) \cdot H_2O$,[8] are also known. Finally, $H_2MnP_3O_{10} \cdot 2H_2O$ has recently been investigated by IR, diffuse-reflectance and X-ray absorption spectroscopies.[9]

As part of our study of phosphates and arsenates of manganese, we describe the synthesis, crystal structure, and a spectroscopic and thermal study of a new manganese(III) arsenate, $MnAsO_4 \cdot 1.2H_2O$. The structure of the thermal decomposition product of $MnAsO_4 \cdot 1.2H_2O$, manganese(II) pyroarsenate, $Mn_2As_2O_7$, has also been refined because a recent study using high-resolution powder neutron data gave a poor profile fit.[10]

Experimental Section

Manganese(III) arsenate hydrate was synthesized by slowly adding H_3AsO_4 (14 mL, 75% w/w in water) to a suspension of 7 g of manga-

(1) (a) Universidad de Málaga, (b) University of Oxford.
(2) Lightfoot, P.; Cheetham, A. K.; Sleight, A. W. *Inorg. Chem.* **1987**, *26*, 3544.
(3) Aranda, M. A.; Bruque, S. *Inorg. Chem.* **1990**, *29*, 1334.
(4) Kampk, A. R.; Moore, P. B. *Amer. Mineral.* **1976**, *61*, 1241.
(5) Bagieu-Beucher, A. *Acta Crystallogr.* **1978**, *B34*, 1443.
(6) Durif, A.; Averbuch-Pouchot, M. T. *Acta Crystallogr.* **1982**, *B38*, 2883.
(7) Lightfoot, P.; Cheetham, A. K.; Sleight, A. W. *J. Solid State Chem.* **1988**, *73*, 325.
(8) Lightfoot, P.; Cheetham, A. K. *J. Solid State Chem.* **1988**, *78*, 17.
(9) Aranda, M. G.; Chaboy, J.; Bruque, S. *Inorg. Chem.*, in press.
(10) Buckley, A. M.; Bramwell, S. T.; Day, P. *J. Solid State Chem.* **1990**, *86*, 1.

0020-1669/91/1330-2043$02.50/0

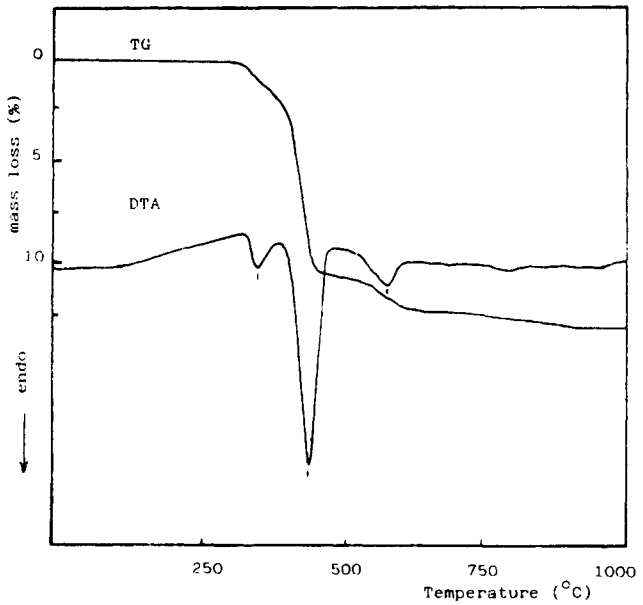

Figure 1. Thermal analysis (TGA and DTA) for $MnAsO_4 \cdot 1.2H_2O$.

nese(II) carbonate hydrate in 20 mL of water. After a release of CO_2, nitric acid (15 mL, 65% w/w in water) was added and the reaction mixture was boiled to oxidize Mn(II) to Mn(III), which resulted in the evolution of NO_2 and the formation of a dark green, polycrystalline precipitate. This was washed with hot water (four times, 20 mL) and oven dried at 100 °C.

The chemical composition was determined by dissolving the solid in boiling concentrated hydrochloric acid and determining the manganese and arsenic contents by atomic absorption spectrophotometry. The water content was measured from the weight change after heating at 800 °C, taking the loss of oxygen when manganese(III) is reduced to manganese(II) into account.

The results and calculated data for the chemical analysis of manganese(III) arsenate hydrate as follows. Anal. Calcd for $MnAsO_4 \cdot 1.2H_2O$: Mn_2O_3, 36.9; As_2O_5, 53.8; H_2O, 9.5. Found: Mn_2O_3, 37.5; As_2O_5, 52.8; H_2O, 9.4.

The oxidation state of the manganese was obtained by dissolving the sample in a solution of potassium iodide and hydrochloric acid. The iodine liberated by the reduction of the manganese to manganese(II) and arsenic(V) to arsenic(III) was titrated with $Na_2S_2O_3$ solution, in the presence of starch. The manganese oxidation state was found to be 2.98.

When $MnAsO_4 \cdot 1.2H_2O$ was heated to 800 °C, a pale pink powder of manganese(II) pyroarsenate, $Mn_2As_2O_7$, resulted. Chemical analysis by the method described above gave the following results. Anal. Calcd for $Mn_2As_2O_7$: MnO, 38.1; As_2O_5, 61.9. Found: MnO, 37.7; As_2O_5, 60.8.

Thermal analysis (TGA and DTA) was carried out in air on a Rigaku Thermoflex apparatus at a heating rate of 10 °C min^{-1} with calcined Al_2O_3 as the reference. Infrared spectra were recorded on a Perkin-Elmer 883 spectrometer using a dry KBr pellet containing 2% of the sample. The diffuse reflectance spectrum (UV–Vis–near-IR) was obtained on a Shimadzu UV-3100 spectrophotometer using an integrating sphere and $BaSO_4$ as the reference blank. X-ray diffraction profiles of the two materials were recorded in 0.02° 2θ steps on a Siemens D501 automated diffractomer by using graphite-monochromated Cu Kα radiation and were transferred to a VAX 8530 computer for analysis. The powder pattern for $MnAsO_4 \cdot 1.2H_2O$ was recorded between 10 and 84° 2θ, counting for 15 s per point; and for $Mn_2As_2O_7$ the pattern was collected in the 2θ range 14–130°, counting for 25 s per step. Rietveld refinements[11] were performed with the program of Wiles and Young[12] using a pseudo-Voigt peak shape function, corrected for asymmetry below 40° in 2θ.

Results and Discussion

$MnAsO_4 \cdot 1.2H_2O$. Thermal Analysis. The water content of samples prepared under differing conditions only varied between 1.1 and 1.2 water molecules per manganese arsenate unit, whereas the phosphate analogue presents a wide range of values for the water content, from 1.0 to 1.5.[2,3,13,14] The TGA–DTA curves for manganese(III) arsenate hydrate are shown in Figure 1. The DTA curve shows three endothermic transformations centered at 340, 425, and 580 °C. The first small endotherm is associated with a loss of weight that corresponds to ≈0.2 water molecules, the second is due to the loss of one water molecule, and the third is associated with the weight loss due to the reduction of manganese(III) to manganese(II) and the consequent release of oxygen. The overall reaction is

$$MnAsO_4 \cdot 1.2H_2O \rightarrow 0.5Mn_2As_2O_7 + 1.2H_2O + 0.25O_2$$

The thermal behavior of manganese(III) arsenate hydrate is different from that of the analogous phosphate, as the reduction of Mn(III) to Mn(II) takes place after the loss of the water molecule, whereas the phosphate is reduced before being dehydrated.[3] In both these of compounds, the loss of water does not begin until 270–290 °C, showing that the water is strongly retained within the structure.

Table I. Final Profile and Structural Parameters for $MnAsO_4 \cdot H_2O$ in Space Group $C2/c$ (No. 15)

Cell Constants

a = 7.0311 (1) Å	V = 380.49 (3) Å^3
b = 7.8250 (2) Å	Z = 4
c = 7.4656 (1) Å	no. of allowed reflcns: 122
β = 112.145 (1)°	no. of points in refinement: 3400

R Factors (%)

R_I = 3.3 R_P = 7.7 R_{WP} = 11.0 R_{EXP} = 3.0

Structural Parameters

atom	sym pos	x	y	z	B, Å^2
Mn	4c	0.2500	0.2500	0.0000	0.83 (6)
As	4e	0.0000	0.4268 (2)	0.2500	0.25 (4)
O(1)	8f	0.4686 (6)	0.2005 (6)	−0.0808 (6)	0.3 (1)
O(2)	8f	0.2885 (7)	−0.0455 (5)	−0.3465 (6)	0.4 (1)
O(3)	4e	0.0000	−0.1052 (10)	0.2500	−0.1 (2)
H	8f	0.083 (9)	−0.037 (8)	0.183 (7)	6 (3)

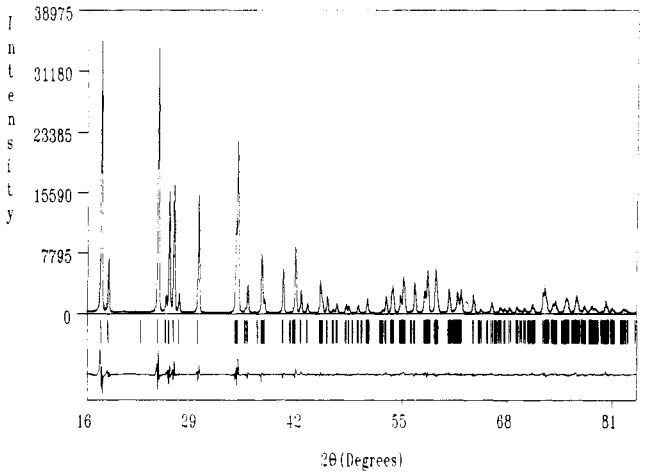

Figure 2. Final observed (points), calculated (full line), and difference X-ray profiles for $MnAsO_4 \cdot H_2O$.

Structure Refinement. The powder pattern of $MnAsO_4 \cdot 1.2H_2O$ was indexed from 20 accurately measured reflection positions by using the Treor program.[15] A C-centered monoclinic cell of dimensions a = 7.030 (1) Å, b = 7.824 (1) Å, c = 7.469 (1) Å, β = 112.14 (1)° was obtained, giving the following figures of merit: M_{20} = 47,[16] and F_{20} = 59 (0.006, 61).[17] This cell is very similar to that of $MnPO_4 \cdot H_2O$, and so the profile was fitted by using the coordinates of this compound as the starting model in space group $C2/c$ with only one water molecule in the structure.[2] In the final refinement, all of the variable coordinates, including those for

(11) Rietveld, H. M. *J. Appl. Crystallogr.* **1969**, *2*, 65.
(12) Wiles, D. B.; Young, R. A. *J. Appl. Crystallogr.* **1982**, *15*, 430.
(13) Narita, E.; Okabe, T. *Bull. Chem. Soc. Jpn.* **1983**, *56*, 2841.
(14) Boyle, F. W.; Lindsay, W. L. *Soil Sci. Soc. Am. J.* **1985**, *49*, 758.
(15) Werner, P. E. *Z. Kristallogr.* **1969**, *120*, 375.
(16) de Wolff, P. M. *J. Appl. Crystallogr.* **1968**, *1*, 108.
(17) Smith, G. S.; Snyder, R. L. *J. Appl. Crystallogr.* **1979**, *12*, 60.

Table II. Bond Distances (Å) and Angles (deg) for $MnAsO_4 \cdot H_2O$

Mn–O(1) × 2	1.891 (5)	O(3)···O(2)	2.667 (6)
Mn–O(2) × 2	1.934 (4)	O(3)–H × 2	1.05 (7)
Mn–O(3) × 2	2.320 (4)	O(2)···H	1.67 (7)
As–O(1) × 2	1.687 (5)		
As–O(2) × 2	1.665 (4)		
O(1)–Mn–O(1)	180	Mn–O(3)–Mn	121.5 (3)
O(1)–Mn–O(2)	94.0 (2)		
O(1)–Mn–O(3)	84.0 (1)	Mn–O(1)–As	135.3 (2)
O(2)–Mn–O(2)	180	Mn–O(2)–As	128.3 (3)
O(2)–Mn–O(3)	92.0 (2)		
O(3)–Mn–O(3)	180	H–O(3)–H	118 (7)
O(1)–As–O(1)	107.6 (3)	O(3)–H···O(2)	157 (4)
O(1)–As–O(2)	110.5 (2)		
O(1)–As–O(2)	107.6 (2)		
O(2)–As–O(2)	112.8 (3)		

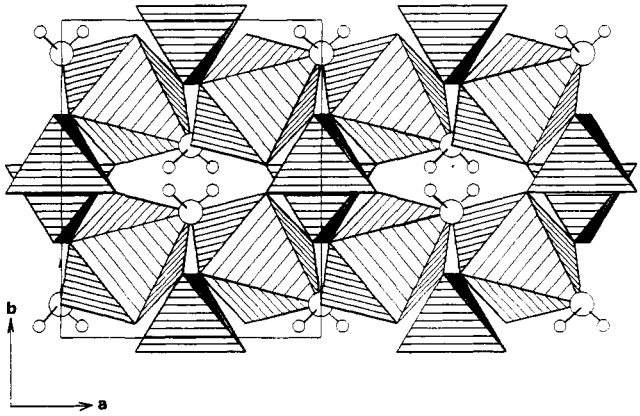

Figure 3. (001) view of $MnAsO_4 \cdot H_2O$.

hydrogen, and isotropic temperature factors were refined independently, giving R_{WP} = 11.0% and R_I = 3.3%. Anisotropic refinement of Mn and As proved possible, but did not improve the fit significantly. Results of the refinement are given in Table I, and the final observed, calculated and difference profiles are given in Figure 2. Final bond distances and angles are given in Table II. These were calculated by using the program ORFFE.[18]

A polyhedral representation (STRUPLO)[19] of the framework of $MnAsO_4 \cdot H_2O$ together with the water molecules is shown in Figure 3. The MnO_6 octahedra are strongly Jahn–Teller distorted, like those in $MnPO_4 \cdot H_2O$,[2] with two long Mn–O bonds to the water molecules that link the octahedra into vertex-sharing chains running parallel to [101]. These are interconnected by AsO_4 tetrahedra, resulting in a three-dimensional network enclosing small channels parallel to *c*. The H atoms of the water molecules project into these tunnels and are hydrogen-bonded to one of the arsenate oxygens, O(2).

The H···O(2) and O(2)···O(3) distances of 1.67 and 2.67 Å are similar to those in $MnPO_4 \cdot H_2O$,[2] which are 1.79 and 2.68 Å, respectively. The O–H distance of 1.05 (7) Å and the HOH angle of 118 (7)° are comparable to those in other hydrates, showing that the hydrogen has been accurately located. It is not clear whether the difference between the stoichiometry of the refined structure, $MnAsO_4 \cdot H_2O$, and the analytical formula, $MnAsO_4 \cdot 1.2H_2O$, is due to the presence of a small amount of amorphous hydrated material or to additional water molecules within the structure that were not located from this refinement. A neutron study will be performed to address this problem.

The observed Mn–O bond distances of 2 × 1.89 Å, 2 × 1.93 Å and 2 × 2.32 Å are similar to found in the Jahn–Teller distorted manganese(III) phosphates, $MnPO_4 \cdot H_2O$,[2] which has 2 × 1.89 Å, 2 × 1.91 Å and 2 × 2.24 Å; $Mn(PO_3)_3$,[5] with 2 × 1.88 Å, 2 × 1.91 Å and 2 × 2.16 Å; $MnHP_2O_7$,[6] with 2 × 1.88 Å, 1.89 Å, 1.97 Å, 2.11 Å and 2.43 Å; and $H_2MnP_3O_{10} \cdot 2H_2O$[9] with 4 × 1.86 Å, 2.09 Å and 2.24 Å.

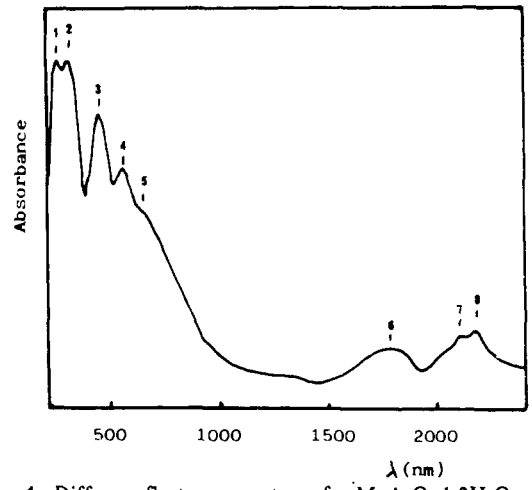

Figure 4. Diffuse-reflectance spectrum for $MnAsO_4 \cdot 1.2H_2O$.

Table III. Diffuse-Reflectance Data for $MnAsO_4 \cdot 1.2H_2O$

band	absorption value, nm	absorption value, cm^{-1}	assignment
1	260	38610	charge transfer
2	320	31250	charge transfer
3	452	22120	$^5B_{1g} \rightarrow {}^5E_g$
4	561	17825	$^5B_{1g} \rightarrow {}^5B_{2g}$
5	655	15150	$^5B_{1g} \rightarrow {}^5A_{1g}$
6	1650–1825	6060–5480	$2\nu(OH)^a$
7	2110	4740	$\nu(OH) + \delta(H_3O^+)$
8	2185	4575	$\nu(OH) + \delta(OHO)$

[a] Set of bands due to combination and overtones of OH stretching vibrations.

Diffuse-Reflectance Study. The diffuse-reflectance spectrum of $MnAsO_4 \cdot 1.2H_2O$ is shown in Figure 4. Five bands are observed in the UV–visible region. Two bands near 259 and 320 nm (Table III) are too strong to be d–d transitions, and lying in the ultraviolet, they are assigned as oxygen to Mn(III) charge-transfer bands. The three bands located in the visible region are explained by the presence of a strong Jahn–Teller effect. Table III lists the absorption maxima values and their assignments. The *Dq* parameter for this compound can be read directly from the spectrum because 10*Dq* coincides with the fourth transition energy $^5B_{1g} \rightarrow {}^5B_{2g}$, giving *Dq* = 1782 cm^{-1}. Similar values are found for other compounds containing Mn(III), e.g. 1770 cm^{-1} for $MnPO_4 \cdot H_2O$,[3] 1790 cm^{-1} for $Mn(acac)_3$, and 1780 cm^{-1} for $[MnF_6]^{3-}$.[20,21] The ground-state splitting (GSS) coincides with the fifth band, and the excited-state splitting (ESS) is the difference between the third and fourth bands. Thus, the GSS assumes a value of 15 150 cm^{-1}, and ESS, a value of 4295 cm^{-1}; these values are very close to those found for $MnPO_4 \cdot H_2O$, which are 15 040 and 4280 cm^{-1}, respectively. The assignments lead to fairly large values of the McClure[22] parameters, $d\sigma$ = −5680 cm^{-1} and $d\pi$ = −2147 cm^{-1}. The well-resolved splitting of the $^5T_{2g}$ state and the high values of *Dq*, $d\sigma$, and $d\pi$ show that Mn(III) is in a tetragonally distorted octahedral environment, in agreement with the crystal structure, with a strong degree of covalence in the Mn–O bonding.

The diffuse-reflectance spectrum in the near-infrared region shows two sets of bands: (i) a very wide band (1600–1850 nm) due to overtones and combinations of the different O–H stretchings and (ii) two partially overlapping bands centered at 2100 and 2185 nm, which correspond to the ν(HO–H) + $\delta(H_3O^+)$ and ν(HO–H)

(18) Busing, W. R.; Martin, K. O.; Levy, H. A. ORFFE. Oak Ridge National Laboratory, Oak Ridge, TN, 1984.
(19) Fischer, R. X. *J. Appl. Crystallogr.* **1985**, *18*, 258.
(20) Lever, A. B. P. *Inorganic Electronic Spectroscopy*, 2nd ed.; Elsevier Science Publishers B. V.: Amsterdam, 1984.
(21) Hush, N. S.; Hobbs, J. M. In *Progress in Inorganic Chemistry*; Cotton, F. A., Ed.; Wiley-Interscience: New York, 1968; p 259.
(22) McClure, D. S. *Advances in the Chemistry of the Coordination Compounds*; Macmillan Co.: New York, 1961.

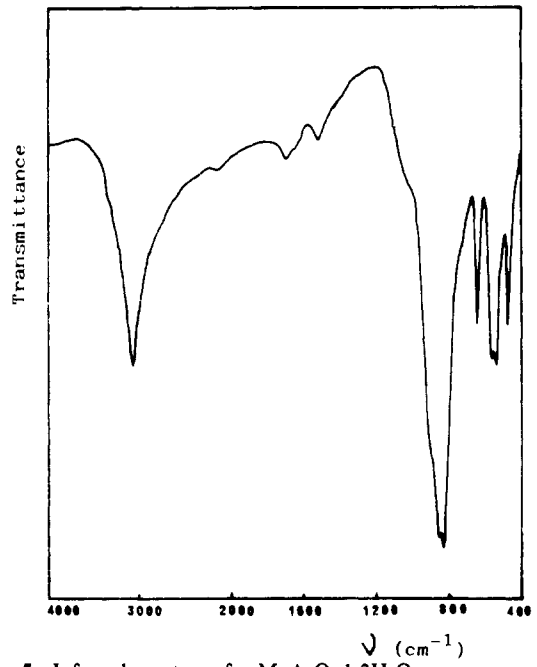

Figure 5. Infrared spectrum for $MnAsO_4 \cdot 1.2H_2O$.

+ δ(O–H–O) combination vibrations, respectively.

Infrared Study. The IR spectrum of $MnAsO_4 \cdot 1.2H_2O$ is shown in Figure 5. The main absorption band in the region of hydroxyl stretching is centered at 3060 cm^{-1} and is assigned to the stretching vibration, ν(O–H), of the strongly hydrogen-bonded water molecule. We previously assigned the corresponding band for $MnPO_4 \cdot 1.3H_2O$ (3110 cm^{-1}) as PO–H stretching,[3] but a careful examination of the literature on infrared studies of hydrogen bonding suggests that this band should be assigned as the stretching O–H vibration of the water molecule when strongly perturbed by hydrogen bonding, ν(O–H···O).

No band can be seen in the H–O–H bending region around 1600 cm^{-1} except for a very weak satellite band, and another, more intense band is observed at 1705 cm^{-1}, which is attributed to the antisymmetric deformation of H_3O^+.[23] The formation of an oxonium ion may be explained if the excess 0.2 water molecules are protonated, consistent with the high temperature at which this water is lost (340 °C). The symmetric deformation of the H_3O^+ ion[24] may be seen as a shoulder at 1050 cm^{-1}, and the stretching vibration of this species appears as a shoulder at 2900 cm^{-1}.[23] A small band of intensity similar to that at 1705 cm^{-1} can be seen at 1520 cm^{-1} and could be associated with in-plane deformation of the O···H···O group.[3]

The absorption bands at 835 and 860 cm^{-1} and the shoulder at ≈900 cm^{-1} are due to splitting of the asymmetric (ν_3) stretching vibration of the AsO_4 groups, which have C_2 symmetry. The first band may also be due to the symmetric (ν_1) stretch, as the low site symmetry makes this band IR-active.[25] The band centered at 640 cm^{-1} is assigned to δ(Mn–O–H), as it disappears on heating when this compound is dehydrated to manganese(II) pyroarsenate, and is very similar to the band found in the phosphate analogue (666 cm^{-1}).[3] The bands centered at 560, 535, and 470 cm^{-1} are assigned to δ(Mn–O–As), ν(Mn–O–As), and $\nu_4(AsO_4)$, respectively.[25,26]

$Mn_2As_2O_7$. Structure Refinement. The powder pattern of $Mn_2As_2O_7$ was indexed on the basis of 20 accurately measured reflection positions by using the Treor program.[15] A *C*-centered monoclinic cell of dimensions a = 6.7493 (8) Å, b = 8.7589 (8) Å, c = 4.7991 (5) Å, β = 102.83 (1)° was obtained, giving the following figures of merit: M_{20} = 58, and F_{20} = 73 (0.005, 51). This unit cell is similar to those of thortveitite ($Sc_2Si_2O_7$)[27] type compounds such as $Mn_2P_2O_7$.[28] The latter structure was used as starting model for a Rietveld refinement in space group *C*2/*m*, which converged to R_{WP} = 6.9%, R_I = 3.2%. A large isotropic temperature factor of 3.7 Å^2 was obtained for the oxygen atom that bridges the pyroarsenate groups, O(1), as has been observed in many thortveitite type structures.[28-31] A carefully study of $Mn_2P_2O_7$[28] has suggested that this is due to a static disorder of oxygens around the ideal O(1) position (0, 0, 0) rather than

Table IV. Final Profile and Structural Parameters for $Mn_2As_2O_7$ in Space Group *C*2/*m* (No. 12)

Cell Constants

a = 6.7563 (1) Å	V = 277.56 (2) Å^3
b = 8.7693 (1) Å	Z = 2
c = 4.8047 (1) Å	no. of allowed reflcns: 157
β = 102.831 (1)°	no. of points in refinement: 5649

R Factors (%)

R_I = 2.9 R_P = 4.9 R_{WP} = 6.7 R_{EXP} = 2.3

Structural Parameters

atom	sym pos	x	y	z	B, (Å^2)	site occ
Mn	4h	0.0000	0.3074 (1)	0.5000	0.56 (2)	1
As	4i	0.2274 (1)	0.0000	−0.0935 (1)	0.60 (1)	1
O(1)	8j	0.0155 (6)	0.0313 (7)	0.0456 (18)	0.62 (4)	0.25
O(2)	4i	0.3939 (4)	0.0000	0.2241 (6)	0.62 (4)	1
O(3)	8j	0.2322 (3)	0.1582 (2)	0.7149 (4)	0.62 (4)	1

Table V. Bond Distances (Å) and Angles (deg) for $Mn_2As_2O_7$

Mn–O(2) × 2	2.168 (2)	As–O(1)	1.730 (6)
Mn–O(3) × 2	2.126 (2)	As–O(2)	1.683 (3)
Mn–O(3) × 2	2.294 (2)	As–O(3) × 2	1.669 (2)
O(2)–Mn–O(3)	152.2 (1)	Mn–O(2)–Mn	102.3 (1)
O(2)–Mn–O(3)	94.3 (1)	Mn–O(3)–Mn	105.7 (1)
O(2)–Mn–O(3)	79.0 (1)		
O(2)–Mn–O(2)	77.7 (1)	Mn–O(2)–As	128.2 (2)
O(3)–Mn–O(3)	115.6 (1)	Mn–O(3)–As	132.6 (1)
O(3)–Mn–O(3)	104.0 (1)	Mn–O(3)–As	118.1 (1)
O(1)–As–O(2)	110.0 (3)	As–O(1)–As	156.5 (4)
O(1)–As–O(3)	109.9 (2)		
O(2)–As–O(3)	114.2 (1)		
O(3)–As–O(3)	112.4 (1)		

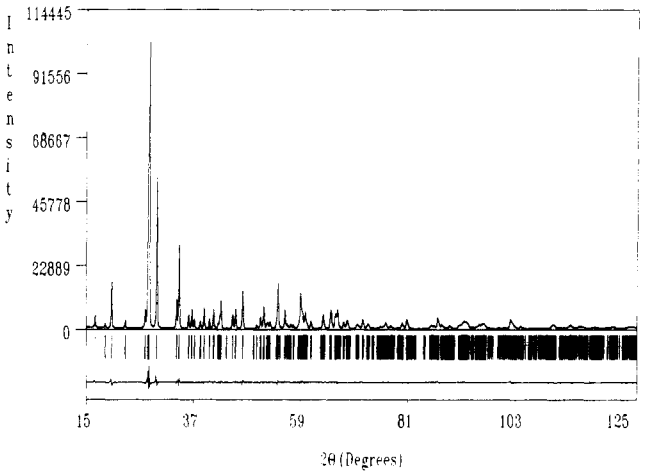

Figure 6. Final observed (points), calculated (full line), and difference X-ray profiles for $Mn_2As_2O_7$.

(23) Remy, P.; Fraissard, J.; Boulle, A. *Bull. Soc. Chim. Fr.* **1968**, 2222.
(24) Tarte, P.; Paques-Ledent, M. T. *Bull. Soc. Chim. Fr.* **1968**, 1750.
(25) Nakamoto, K. In *Infrared Spectra of Inorganic and Coordination Compounds*, 4th ed.; Wiley, J. S., Ed.; Wiley-Interscience: New York, 1986.
(26) Ross, S. D. In *The Infrared Spectra of Minerals*; Farmer, V. C., Ed.; Mineralogical Society: London, 1974.
(27) Zachariasen, W. H. *Z. Kristallogr.* **1930**, *73*, 1.
(28) Stefanidis, T.; Nord, A. G. *Acta Crystallogr.* **1984**, *C40*, 1995.
(29) Cruickshank, D. W. J.; Lynton, H.; Barclay, G. A. *Acta Crystallogr.* **1962**, *15*, 491.
(30) Dorm, E.; Marinder, B. O. *Acta Chem. Scand.* **1967**, *21*, 590.
(31) Robertson, B. E.; Calvo, C. *Can. J. Chem.* **1968**, *46*, 605.

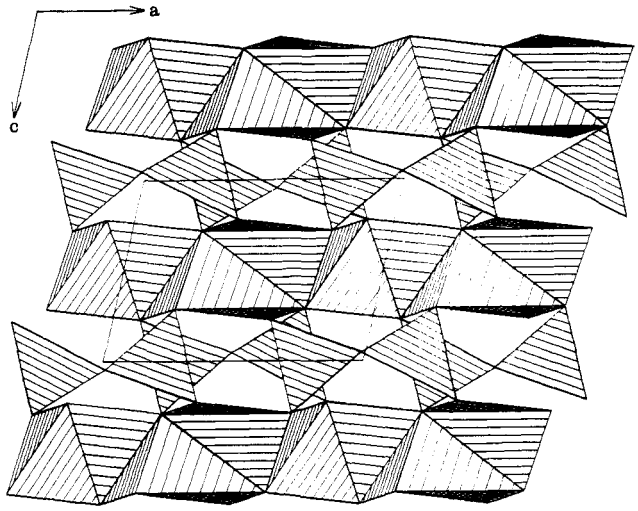

Figure 7. (010) view of $Mn_2As_2O_7$.

thermal vibrations. Refinements in $C2/m$ with O(1) on (0, y, 0) to give a nonlinear As–O–As bond improved the fit, but B[O(1)] was still larger than the other oxygen temperature factors, whereas refining O(1) freely on (x, y, z), gave in an unrealistic large negative value for B[O(1)]. Finally we attempted to model the disorder in $Mn_2As_2O_7$ in a chemically realistic way by refining O(1) off (0, 0, 0) subject to the constraints that this atom must remain equidistant from the two As atoms and that the isotropic temperature factors of all the oxygen atoms are equal. This gave a good fit (R_{WP} = 6.7%, R_I = 2.9%), and the results are shown in Tables IV and V. The observed, calculated, and difference profiles are displayed in Figure 6.

Figure 7 shows a polyhedral representation of the thortveitite type structure of $Mn_2As_2O_7$, which consists of layers of edge-sharing MnO_6 octahedra linked by pyroarsenate groups. The disorder of the oxygen atoms that bridge the pyroarsenate groups has been represented by placing each bridging oxygen in one of the four available O(1) sites at random. The values of the As–O(1) distance, 1.730 (6) Å, and the As–O(1)–As angle, 156.5 (4)°, are quite plausible as pyroarsenate groups may be highly bent; e.g., $Na_4As_2O_7$,[32] has the distance As–O(1) = 1.783 Å and the angle As–O(1)–As = 123.5°.

Infrared Study. The IR spectrum for $Mn_2As_2O_7$ is shown in Figure 8. The main characteristic is the band that appears at 985 cm^{-1}, which is due to the stretching vibration of the pyroarsenate bridge, As–O–As. The asymmetric stretching vibration of AsO_4 tetrahedra can be seen at 855 cm^{-1}, and the band at 820 cm^{-1} may be assigned to a splitting of this vibration or to the symmetric stretching vibration of the AsO_4 group or both. The broad band centered at 470 cm^{-1} is assigned to $\nu_4(AsO_4)$ although it may also include δ(Mn–O–As) and ν(Mn–OAs).

Conclusions

Novel manganese(III) arsenate hydrates, $MnAsO_4 \cdot nH_2O$, with n = 1.1–1.2 can be synthesized as polycrystalline precipitates. A Rietveld refinement of the structure of $MnAsO_4 \cdot 1.2H_2O$ using X-ray powder diffraction data shows that this compound adopts the $MnPO_4 \cdot H_2O$ structure type, but whether the additional 0.2

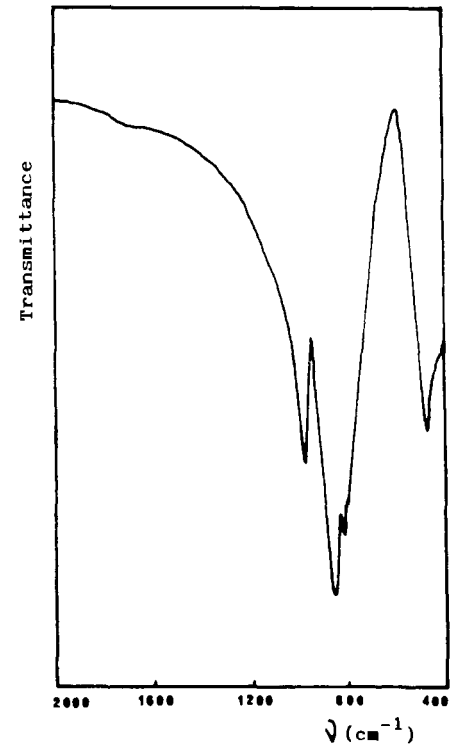

Figure 8. Infrared spectrum for $Mn_2As_2O_7$.

water molecules are present in the structure or in a second amorphous phase is unclear. Mn^{3+} is in a tetragonally Jahn–Teller distorted octahedral environment, and the diffuse-reflectance spectrum has been used to quantify the splittings of the d states. Even the H position has been refined without constraints, enabling the hydrogen-bonding geometry to be calculated. Although $MnAsO_4 \cdot H_2O$ is isostructural with $MnPO_4 \cdot H_2O$, their thermal decomposition pathways differ, as water is lost from the arsenate before reduction to $Mn_2As_2O_7$ takes place, whereas the phosphate is reduced before being dehydrated. This may reflect the larger channels in the arsenate allowing diffusion of water to take place more readily than in the phosphate.

The split model used to model the disorder of the bridging oxygen in $Mn_2As_2O_7$ gives a good fit to the X-ray data and provides a realistic description of the structure, as a bent configuration is electronically more stable than a linear one for pyro groups. It is notable that even the precision in the refined oxygen parameters is slightly better than that in the previously reported high-resolution neutron study,[10] demonstrating that a good peak shape description is vital for profile fitting.

The two Rietveld refinements also show that good structural descriptions may be obtained with data from laboratory diffractometers of moderate resolution (minimum full width at half maximum = 0.15°). Collecting data over a large 2θ range with long count times enables subtle features such as the H position in $MnAsO_4 \cdot H_2O$ and the disorder in $Mn_2As_2O_7$ to be determined.

Acknowledgment. We thank the British Council and Ministerio de Educacion y Ciencia (Spain) for funding from the Acciones Integradas Programme. M.G.A. thanks the Spanish Government for a Studentship and J.P.A. thanks Christ Church, Oxford, U.K., for a Junior Research Fellowship.

(32) Leung, K. Y.; Calvo, C. *Can. J. Chem.* **1973**, *51*, 2082.